



# Monitoring land use and land cover change near a nuclear power plant construction site: Akkuyu case, Turkey

Muzaffer Can Iban · Ezgi Sahin

Received: 7 March 2022 / Accepted: 30 August 2022 / Published online: 3 September 2022  
© The Author(s), under exclusive licence to Springer Nature Switzerland AG 2022

**Abstract** Land use and land cover (LULC) change analysis of the construction site and its surroundings of the Akkuyu Nuclear Power Plant project in southern Turkey was undertaken in this case study, which was supported by remotely sensed Landsat 8 image composites. The composite images compiled in 2017 and 2021 were prepared on the Google Earth Engine platform. The Random Forest algorithm was used as the classifier model. A high classification performance was obtained for both images ( $\kappa > 0.88$ , overall accuracy  $> 90\%$ ). After the classification process, LULC maps for both years were generated, and statistical calculations for the LULC change were computed for both the entire study area ( $15 \times 25 \text{ km}$ ) and a buffer zone with a radius of 1 km around the power plant. In the whole study area, artificial surfaces significantly increased (78.46%), whereas forests ( $-8.31\%$ ) and barren lands experienced a considerable decrease ( $-6.11\%$ ). In the 1 km buffer, artificial surfaces predominantly increased (113.94%), while forests and barren lands decreased dramatically

( $-69.13\%$  and  $-74.28\%$ , respectively). The agricultural areas in the study area were changed into other LULC classes: 9.1% to artificial surfaces, 27.6% to barren lands, and 21.7% to forest. The rise in the area of artificial surfaces was especially noticeable within the 1 km buffer zone: construction activities converted 36.1% of agricultural fields, 54.1% of forests, and 23.2% of barren lands into artificial surfaces. The filling activities on the seashore resulted in a loss of water bodies of up to 26.5%. The study provides an overview of how the LULC classes have evolved on the construction site and in the region. In the end, the study discusses how the current land use preferences in the region contradict the issues and concerns mentioned in the existing body of literature.

**Keywords** Google earth engine · Land use land cover · Nuclear power plants · Random forest · Remote sensing

## Introduction

Although the Fukushima nuclear disaster in 2011 has had a significant influence on nuclear energy development in recent years, nuclear energy, as a low-carbon energy source, is presently an alternative energy source that can be produced on a large scale. Despite a modest decline in nuclear output after Fukushima, nuclear power generation has continued to increase in recent

M. C. Iban (✉)  
Department of Geomatics Engineering, Mersin University,  
Çiftlikköy Campus, Mersin 33343, Türkiye  
e-mail: caniban@mersin.edu.tr

E. Sahin  
Department of Geographic Information Systems  
and Remote Sensing, Mersin University, Çiftlikköy  
Campus, Mersin 33343, Türkiye  
e-mail: ezgisahin.9600@gmail.com

years, making a rising contribution to the world's supply of clean and dependable energy (Xu et al., 2021).

Many researchers have conducted systematic studies on the environmental impact assessment (Bond et al., 2004; Lee et al., 2018; Salter et al., 2012) and site selection of Nuclear Power Plants (NPPs) (Abudeif et al., 2015; Erdogan & Kaya, 2016; Kirkwood, 1982), nuclear waste disposal areas (Bilgilioğlu, 2022; Rezaeimahmoudi et al., 2014), and the recreation of the site after the shutdown of an NPP (Lee et al., 2021; Pasqualetti & Pijawka, 1996; Yamamoto et al., 2020). However, monitoring LULC change and its prospective effects during and after the construction of any NPP has not been a popular topic studied by researchers.

Monitoring LULC changes enables scientists to get a picture of the interconnection between natural geography and human activities. Once humanity rules over the natural environment, such inhabited areas become more populated and the dynamics of the natural environment change significantly (Foley, 2005; Song et al., 2018; Turner et al., 2007). Geographic information systems (GIS) and remote sensing (RS) are functional tools for determining the spatial and temporal changes in LULC of any area. RS products provide a wide range of multi-temporal data for examining LULC changes over a certain period, while GIS software packages help to map and analyze these changing patterns (Hawash et al., 2021; Prabu & Dar, 2018).

The preceding case studies on LULC served a variety of goals. However, the principal goal of recent works was to track the land use changes (Aksu & Iban, 2019; Fallati et al., 2017; Kharazmi et al., 2018). Other goals have been determining the drivers of LULC change (Doygun & Alphan, 2006; Kindu et al., 2015), estimating urban sprawl (Akin et al., 2015; Sekertekin et al., 2018; Wu et al., 2016; Yin et al., 2011), monitoring deforestation, ecosystem services, and agricultural land loss (Çakir et al., 2008; Dubovyk et al., 2013; Hu et al., 2008; Lele & Joshi, 2009), and delineating the changes along the coastlines (Qiang & Lam, 2015; Sesli et al., 2009). Some studies work on a global scale, while some cases are interested in a national or regional context. Some LULC change studies focus on smaller sites such as national parks (Kidane et al., 2012), basins (Zadbagher et al., 2018), or protected areas (Sano et al., 2010).

The research of LULC change relies heavily on RS products. Remotely sensed image classification is regarded as a key activity in image processing and

is therefore employed in the extraction of knowledge from LULC data by classifying the spectral signs (Dewan & Yamaguchi, 2009; Eisavi et al., 2015). Thematic mapping of LULC is derived from image classification with the help of software and visual interpretation. Images are commonly classified by labelling their pixels in order to obtain a classifier model. The case studies related to image classification have used supervised and unsupervised approaches. Unsupervised approaches can be listed as K-means clustering (Lv et al., 2019; Celik, 2009), Iterative Self-Organizing Data Analysis (ISODATA) clustering (Güler et al., 2007), K-mean clustering (Kusak et al., 2021), and Fuzzy C-means clustering (Adhikary et al., 2019). On the other hand, maximum likelihood (Karan & Samadder, 2016; Mahdavi Saeidi et al., 2020), k-nearest neighbor (Chirici et al., 2016; Yadav & Nandy, 2015), Mahalanobis distance (Yousefi et al., 2015), Classification and Regression Trees (CART) (Shao & Lunetta, 2012; Shetty, 2019), Support Vector Machines (SVM) (Huang et al., 2002; Kavzoglu & Colkesen, 2009), and Random Forest (RF) (Ghosh et al., 2014; Pal, 2005) classifiers have been popular supervised approaches. The basis for determining LULC change lies in the calculation of the differences between the pixel reflectance values of two images obtained on different dates. In order to identify LULC changes, the pixels in the images need to be classified in accordance with their LULC classes (Lu et al., 2004). Hence, it is easier to compare and detect LULC changes between two LULC maps.

LULC change analyses for other types of power plants have been put into practice by researchers, and it has been proven that such analyses help measure the impact of power plants on the natural and built environment. For instance, Guerrero et al. (2020) monitored the deforestation processes around a hydropower complex in the Amazon forests over 33 years. Singh et al. (1997) monitored the land use patterns nearby a thermal power plant in central India. Hernandez et al. (2015) evaluated potential land cover change resulting from the development of photovoltaics and power systems within California. Even though there are a vast number of studies on radioecological monitoring of terrestrial and aquatic environments in the vicinity of NPPs, there are very few case studies that analyze LULC trends. For instance, Gemitz (2020) monitored long-term radiation effects on vegetation phenology after the closure of Chernobyl NPP using

satellite-borne LULC data. Sah et al. (2012) put forward the importance of LULC maps for assisting emergency response in the case of nuclear accidents and implemented an LULC map generation for the Nine Mile Point NPP in the USA. Manfré et al. (2020) sought potential evacuation routes using Sentinel 2A imagery and GIS for the Angra dos Reis NPP in Brazil. Two recent studies from Turkey addressed the deforestation and vegetation loss in the vicinity of the Sinop NPP construction area using remotely sensed products and vegetation indices (Çolak et al., 2021; Sabuncu, 2020). Such examples underline the importance of monitoring LULC changes around NPPs to detect environmental aspects and human activities during their operating life.

This study tracks the LULC changes surrounding the Akkuyu NPP, which is under construction now in the south of Turkey, with the help of the classification of multi-temporal remotely sensed data. In the second section, a literature review on the LULC policies and preferences around NPPs is presented, and the background of the Akkuyu NPP project and related LULC policies are introduced. In the third section, the study area and its extent are demonstrated. In the fourth section, information about the datasets used in the study, the classification scheme of satellite images, accuracy assessment, and LULC change analysis are given. In the fifth section, the quantitative and comparative results of the LULC change analysis are demonstrated. LULC maps for the years 2017 and 2021 are presented, and the LULC change is illustrated to shed light on how the Akkuyu NPP project increases the use of land for built-up spaces and negatively affects the natural land cover. The sixth section discusses how the current land use preferences in the region contradict the issues and concerns mentioned in the existing body of literature.

## Background

The construction of NPPs has a consequential impact on the terrestrial and marine environment. Even though NPPs do not require a massive land area for energy production, just like hydropower, solar, and wind energy (NEI, 2015), the terrestrial environment is cleared during construction. Such clearance can result in deforestation and the loss of barren and agricultural lands (Barthouse, 2013). Moreover, for the

facilities of an NPP, seashores can be filled with reinforced concrete, resulting in a loss in the water body area.

Destroyed vegetation (agricultural and barren lands, forests) must be taken into account in the first place, as it can lead to erosion, local pollution, and a decrease in groundwater sources (Odum, 1976). A loss of arable land resulting from the construction of an NPP can occur, and the economic activities near the NPP can be contaminated by radioactive elements. Therefore, food production, industrial activities, and harbors are not desirable in the areas close to NPPs. Moreover, NPP sites near the sea are considered better for the effluent water treatment process. In contrast, any site nearby a freshwater source is not desirable due to potential contamination (Janssen, 1984).

The construction of NPPs has an impact on built-up areas and the local population. An increase in the population densities around NPPs can occur due to the influx of labor forces (Janssen, 1984). Managing and controlling the projected population growth occurring around an operating NPP is crucial as an effective evacuation plan is required in the event of a nuclear accident (Nero et al., 1977). Therefore, the population and built-up areas around NPPs should not exceed the specified limit indicated by national guidelines (Janssen, 1984; Nero et al., 1977).

Turkey is one of the countries that still intends to benefit from nuclear power without revising its original plans despite the Fukushima and Chernobyl disasters. The central government has been coordinating the planning and installation of NPPs as a step forward in energy independence and scientific advancement. Turkey intends to set up three NPPs that are expected to meet 15% of its electricity needs (Hickey et al., 2021). In the 1970s, the Akkuyu Bay, which is located on the eastern Mediterranean coast in the province of Mersin, was selected for the construction of the first Turkish NPP. However, due to a failure to take proper actions for law-making and tender processes, the construction could not begin until a bilateral deal was signed between the Russian and Turkish administrations. A company called Rosatom will install and operate four units, each with a capacity of 1200 MW, at the Akkuyu NPP. After this deal was signed, the bureaucratic processes were completed (Ağbulut et al., 2019; Aydin, 2020; Melikoglu, 2016). An updated site investigation was conducted by the

Akkuyu Project Company (APC) in 2011 and the produced report was reviewed and approved by the Turkish Energy, Nuclear and Mining Research Authority and the International Atomic Energy Agency (IAEA). Then, the environmental impact assessment report for the project was prepared and submitted by the APC. The Turkish Ministry of Environment and Urbanization approved this assessment report in 2013 (IAEA, 2020). Finally, the construction began in April 2018 (Thomas, 2018).

According to the IAEA's guide (IAEA, 2015), several emergency zones should be established where arrangements are made in order to "*reduce the risk of severe deterministic health effects before and shortly after the release of any radioactive material.*" These zones cover a buffer area around the construction site within a radius of 5 to 20 km. Similarly, the National Radiation Emergency Plan (URAP) (2019) prepared by the Turkish Ministry of Interior–Disaster and Emergency Management Presidency cites the same emergency zones; however, the URAP does not indicate the projected land use and population around the Akkuyu NPP.

The Environmental Land Use Plan (ELUP) at a scale of 1:100000 covering the provinces of Mersin and Adana was entered into force in 2018 and has been updated 18 times so far. This plan also covers the Akkuyu NPP construction area. The ELUP does not contain any statement about controlling the LULC around the Akkuyu NPP. The expected policy outcome should be to limit new development that may attract migration and keep the population density below a certain level in the region. Paradoxically, the plan shows that large-scale development areas, which may lead to a significant population rise, are planned for the rural settlements in the region. The ELUP does not suggest any method that limits the number of residential units for prospective employees. Instead, it seems that the government is addressing new development areas around rural villages to supply the housing needs of the labor force. The Akkuyu Region is sparsely populated, and the main driver of the regional economy is agricultural production. Nonetheless, the land use decisions taken in the ELUP will accelerate urbanization in the region. Furthermore, the APC states that they will monitor the environment during the construction and help to reclamate and revegetate the land affected by the construction. However, neither the APC nor the Turkish government indicates the

amount of land surface that will be used for construction and be affected by the NPP. Thus, it can be said that this study will help determine this unexplained land use amount by applying RS techniques.

## Study area

The Akkuyu NPP study area is located in the province of Mersin in southern Turkey, at the coordinates of 36°08' N and 33°32' E (Fig. 1). The closest urban areas to the Akkuyu NPP are the district of Silifke, which is approximately 30 km away from the study area and has a current population of approximately 125 thousand, and the district of Gülnar, which is approximately 20 km away from the study and has a current population of approximately 25 thousand. The Akkuyu region is limited to the south by the Mediterranean Sea, to the north by the Taurus Mountains, and to the west by Antalya. Cyprus Island is around 100 km to the south, while the main metropolitan areas of Damascus and Beirut are about 300–400 km away.

Various studies have stated the reasons why Akkuyu was selected for the first NPP in Turkey. Among these is the fact that Akkuyu is seismically stable and located on the seashore, provides appropriate transportation and cooling water, and is significantly less populated, making it safer in case of any accidents (Aydın, 2020; Küçükoğlu, 2020). A sensitivity analysis conducted by Ekmekçioğlu et al. (2011) concluded that Akkuyu was the second-best place, after Sinop, to construct an NPP among the other alternative sites.

According to IAEA's guide (2015), two off-site emergency zones should be established: the first one, namely the precautionary action zone (PAZ), where arrangements are taken in order to "*reduce the risk of severe deterministic health effects before and shortly after the release of any radioactive material,*" and the second one, namely the urgent protective action planning zone (UPZ), where arrangements are taken to "*reduce the negative effects of the radioactive dose.*" The Akkuyu NPP is a category 1 facility and will have four reactors that produce more than 1000 MW. IAEA's guide suggests approximate distances for such reactors (3–5 km for PAZ, 5–30 km for UPZ); however, there is no crystal-clear definition of how to select these distances in the IAEA's guide or the National Radiation Emergency Plan (URAP) prepared by the Turkish Ministry of Interior–Disaster and



**Fig. 1** Study area

Emergency Management Presidency (2019). Therefore, in order to test the suggested methodology and evaluate the results, a rectangular area with  $15 \times 20$  km dimensions, whose center is overlaid with the construction site, is selected for the LULC monitoring. This study area covers the PAZ and UPZ addressed in the IAEA guides, a new highway being constructed nearby the project site, and the new development areas planned in the ELUP near Akkuyu. For NPPs, there is an exclusionary zone which is under effective control

of the plant management, and public habitation is prohibited within this zone (IAEA, 2015). Therefore, it is important to evaluate the LULC changes around the construction. On the contrary, it is equally critical to assess how the construction alters the land footprint over time. Since the APC did not specify the size of the construction, we opted to focus on a buffer circle with a radius of 1 km. This smaller area in the core of the construction was subjected to a separate LULC analysis.

## Materials and methods

The goal of this study is to identify LULC changes around the Akkuyu NPP construction site by classifying remotely sensed images. The workflow consists of four steps: selecting the images, classifying the images, accuracy assessment in Google Earth Engine, and LULC change analysis (Fig. 2).

For image selection and supervised classification, the Google Earth Engine (GEE) was used. GEE is a cloud-based web platform for geospatial tasks. It

takes advantage of Google's extensive computational expertise for numerous Earth monitoring activities. The main advantages of GEE are that it provides multi-petabyte data, GIS functionality, built-in RS and machine learning (ML) algorithms, an online code editor and visualization, and cloud processing. The GEE is in charge of many of the issues that arise when it comes to data storage, cataloguing, and projection. Many of the most common RS data sources have been absorbed by GEE (Gorelick et al., 2017; Sazib et al., 2018; Shelestov et al., 2017).

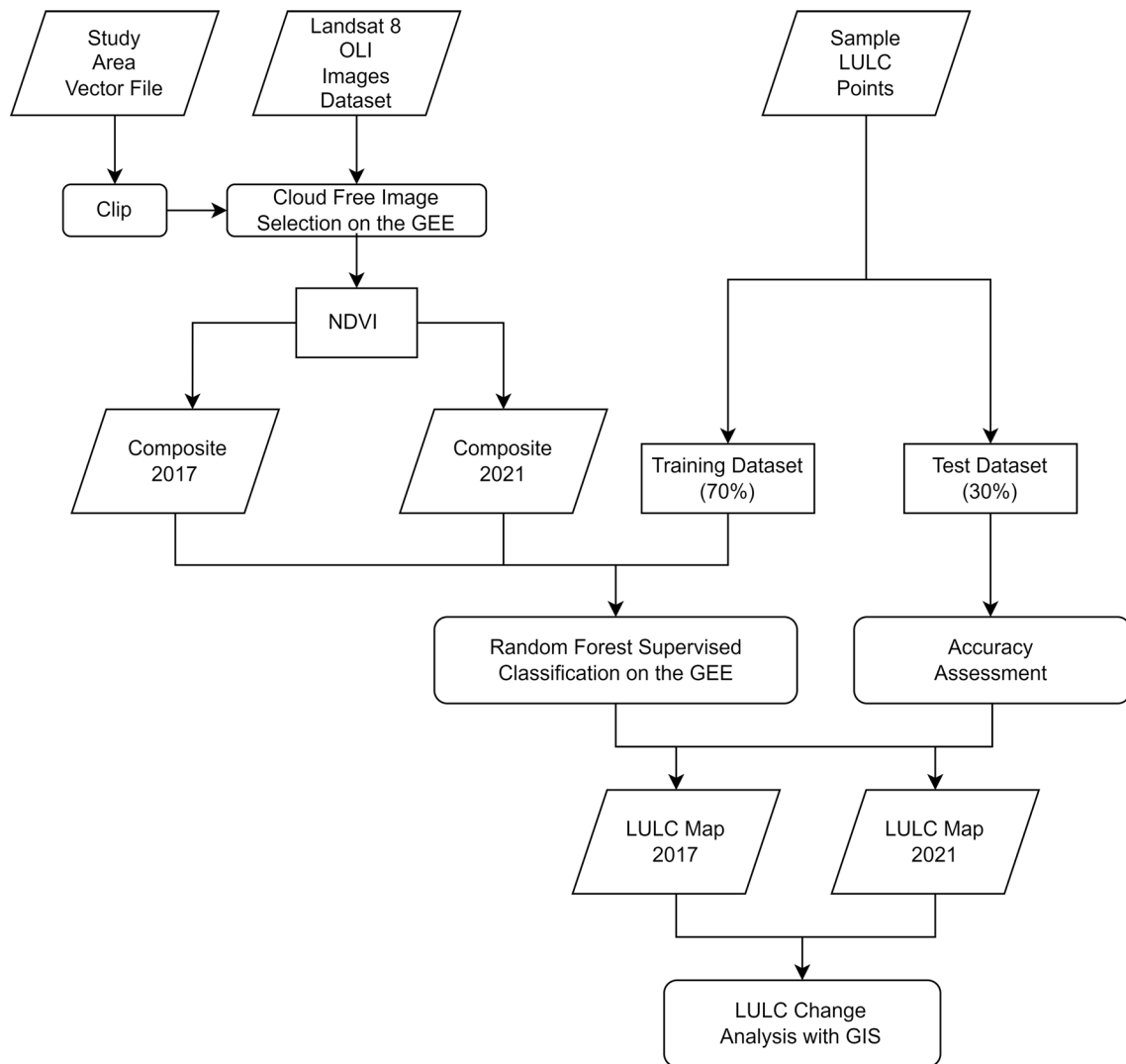


**Fig. 2** The flowchart of the generated LULC maps

## Data used

The study area was delimited by uploading a vector file as an input to the GEE. Then, we chose Landsat 8 (L8) atmospherically corrected surface reflectance scenes accessible on the GEE platform for the year 2017 (before construction began) and the year 2021 in order to delineate the LULC change between these 2 years and evaluate the impact of the construction of Akkuyu NPP. These multi-temporal composites were created using the filtered collection by date function (*filterDate*) on the GEE platform. Both composites cover the summer period between May 1 and September 30, as this is the time of year when different kinds of vegetation are all at a stable stage.

As part of NASA's Landsat Data Continuity Mission (LDCM), the L8 Operational Land Imager (OLI) generates RS data that is consistent with previous Landsat projects. Medium-resolution Landsat datasets allow LULC analyses across long time scales. L8 offers multi-spectral imagery with a 30-m spatial resolution, 5 visible and near-infrared bands, and 2 short-wave infrared bands, with a revisit period of 16 days (Tassi & Vizzari, 2020). At the atmospherically surface reflectance (SR) processing level, 30-m L8 bands are now accessible in GEE.

A vital stage in every LULC classification is the preparation of the basis dataset. The compilation of this dataset for the L8 data in this study begins in the GEE with a filtered and cloud-masked image collection. Visible and infrared bands of L8 images, as seen Table 1, are used to form false color images to be used in placing training pixels. Then, for each image in the collections, the Normalized Difference Vegetation Index (NDVI) is calculated. The NDVI is frequently employed to map the changes in LULC, and it improves classification accuracy significantly. The NDVI ranges between -1 and +1. These values also help to select training samples since negative values

generally correspond to water bodies, while barren lands and artificial surfaces fall between 0 and 0.2. NDVI values of more than 0.2 usually show the areas covered with healthy vegetation (Sims & Gamon, 2002). The NDVI is calculated with the formula of  $(NIR-R)/(NIR+R)$  where NIR corresponds to the Near-Infrared Band 5 of L8, and R denotes the Red Band 4 of L8 (Li et al., 2013). Hence, we selected R and NIR bands of L8 and generated the NDVI values as the dependent variable in the classification task. The composite images of both years consist of NDVI values derived from Red and NIR bands. For the composition of the dataset, the maximum percent of cloud cover was set to 10. However, remaining cloudy and no-data pixels were identified by *cfmask* band from SR collection to get an output with cloud mask. The composition consists of 11 images from 2017, and 20 images from 2021 (path 176 — row 35 and 36) (Table 2). The resulting single image composites were composed of the median NDVI values of all the pixels in the images in the filtered collection at that location.

## Classification scheme

The classification scheme is interested in five LULC classes: (1) artificial surfaces, including settlements, lands covered by concrete, and all sorts of built-up areas; (2) agricultural areas, including annual and permanent crops, grasslands, and greenhouses; (3) forests; (4) water bodies, including the sea and streams; and (5) barren lands, including lands having few plants, sandy, and rocky areas.

Satellite image classification aims to automatically classify each pixel into LULC classes. However, supervised image classification requires a priori knowledge of the LULC classes of interest. The selected LULC classes need to be marked on the images for training the supervised classification algorithms. Hence, we collected a total of 2000 randomly distributed pixels throughout both composite images in the GEE environment. This sample set is randomly split into 1400 training pixels (70% of the samples and 280 samples per class) and 600 validation (test) pixels (30% of the samples and 120 samples per class). The training pixels were used for training the classifier, and the remaining validation pixels were used for assessing the performance of the classification. The selection of these pixels was based on a visual approach supported

**Table 1** Used L8 bands

Name	Description	Wavelength	Spatial resolution (m)
Band 2	Blue SR	0.452–0.512 μm	30
Band 3	Green SR	0.533–0.590 μm	30
Band 4	Red SR	0.636–0.673 μm	30
Band 5	NIR SR	0.851–0.879 μm	30

**Table 2** L8 images used

Image ID	Path	Row	Acquisition date	Season in the region
LC08_L2SP_176036_20170915_20200903_02_T1	176	35	September 15, 2017	Summer
LC08_L2SP_176036_20170830_20200903_02_T1	176	36	August 30, 2017	Summer
LC08_L2SP_176036_20170814_20200903_02_T1	176	36	August 14, 2017	Summer
LC08_L2SP_176036_20170729_20200903_02_T1	176	36	July 29, 2017	Summer
LC08_L2SP_176036_20170713_20200903_02_T1	176	36	July 13, 2017	Summer
LC08_L2SP_176036_20170526_20200903_02_T1	176	36	May 26, 2017	Spring
LC08_L2SP_176036_20170510_20200904_02_T1	176	36	May 10, 2017	Spring
LC08_L2SP_176035_20170830_20200903_02_T1	176	35	August 30, 2017	Summer
LC08_L2SP_176035_20170814_20200903_02_T1	176	35	August 14, 2017	Summer
LC08_L2SP_176035_20170729_20200903_02_T1	176	35	July 29, 2017	Summer
LC08_L2SP_176035_20170713_20200903_02_T1	176	35	July 13, 2017	Summer
LC08_L2SP_176036_20210926_20211001_02_T1	176	36	September 26, 2021	Autumn
LC08_L2SP_176035_20210926_20211001_02_T1	176	35	September 26, 2021	Autumn
LC08_L2SP_176036_20210910_20210916_02_T1	176	36	September 10, 2021	Summer
LC08_L2SP_176035_20210910_20210916_02_T1	176	35	September 10, 2021	Summer
LC08_L2SP_176036_20210825_20210901_02_T1	176	36	August 25, 2021	Summer
LC08_L2SP_176035_20210825_20210901_02_T1	176	35	August 25, 2021	Summer
LC08_L2SP_176036_20210809_20210819_02_T1	176	36	August 9, 2021	Summer
LC08_L2SP_176035_20210809_20210819_02_T1	176	35	August 9, 2021	Summer
LC08_L2SP_176036_20210724_20210730_02_T1	176	36	July 24, 2021	Summer
LC08_L2SP_176035_20210724_20210730_02_T1	176	35	July 24, 2021	Summer
LC08_L2SP_176036_20210708_20210713_02_T1	176	36	July 8, 2021	Summer
LC08_L2SP_176035_20210708_20210713_02_T1	176	35	July 8, 2021	Summer
LC08_L2SP_176036_20210622_20210629_02_T1	176	36	June 22, 2021	Summer
LC08_L2SP_176035_20210622_20210629_02_T1	176	35	June 22, 2021	Summer
LC08_L2SP_176036_20210606_20210615_02_T1	176	36	June 6, 2021	Spring
LC08_L2SP_176035_20210606_20210615_02_T1	176	35	June 6, 2021	Spring
LC08_L2SP_176036_20210521_20210529_02_T1	176	36	May 21, 2021	Spring
LC08_L2SP_176035_20210521_20210529_02_T1	176	35	May 21, 2021	Spring
LC08_L2SP_176036_20210505_20210517_02_T1	176	36	May 5, 2021	Spring
LC08_L2SP_176035_20210505_20210517_02_T1	176	35	May 5, 2021	Spring

by high-resolution Bing and Google Earth images, L8 NDVI profiles, false color composites, and local LULC maps.

The confusion matrix method, which is a widely used approach for comparing classification outputs with validation data, was used to analyze the performance of the classifier. The confusion matrix can be used to derive some specific accuracy measures: overall accuracy (OA, Eq. 1), producer's accuracy (PA, Eq. 2), and user's accuracy (UA, Eq. 3). The OA corresponds to the total efficacy of the classifier. The PA (also known as recall) can be defined as the power of

the algorithm to detect positive labels. The UA (also known as precision) gives the consistency between the input and the positive labels detected by the algorithm. When a classifier achieves a high recall and precision value, it is considered very accurate. High precision (UA) corresponds to a low number of commission errors, while high recall (PA) leads to a low number of omission errors in the LULC classification.

$$OA = \frac{\text{The number of correctly classified samples}}{\text{The total number of samples}} \quad (1)$$

$$PA = \frac{\text{The number of correctly classified samples of a particular class}}{\text{The total number of samples of the same class}} \quad (2)$$

$$UA = \frac{\text{The number of correctly classified samples of a particular class}}{\text{The total number of classified samples in the same class}} \quad (3)$$

The last metric we used is Cohen's kappa coefficient (Eq. 4). Cohen's kappa is a common statistic for determining how well the predicted and observed classes agree, calculated as follows:

$$\kappa = \frac{p_0 - p_e}{1 - p_e} \quad (4)$$

where  $p_0$  is the relative observed agreement in the classifier, and  $p_e$  is the hypothesized probability of change agreement. It basically tells how much better the classifier performs than a classifier that predicts randomly based on the class frequency. The Cohen's kappa coefficient is always less than or equal to one. A number of 0 indicates no agreement, 0.21–0.40 is reasonable, 0.41–0.60 is moderate, 0.61–0.80 is considerable, and 0.81–1 is nearly faultless agreement.

The classifier package of GEE administers supervised image classification by so-called ML algorithms. These ML classifiers are SVM, CART, Naïve Bayes, gradient tree boost, and RF. We used the RF classifier to accomplish our LULC classification task. So far, RF is one of the most commonly used ML classifiers for LULC classification using remote sensing data. The RF classifier handles outliers and noisier datasets as well as it has shown good performance with high dimensional input data (Phan et al., 2020). According to several applications, its classification accuracy outperformed the other classifier algorithms. Moreover, the RF algorithm has shown a relatively higher processing speed than other classifiers used. RF has more hyperparameters to tune; thus, the classifier can be trained in a more optimized way. According to a recent review scanning through 349 articles on GEE, the RF classifier is the most preferred method for satellite image classification (Tamiminia et al., 2020).

#### LULC mapping and change detection

The LULC maps of the study area were produced using the RF classification approach for two different Landsat composites. In order to assess the LULC

change between the years 2017 and 2021, the post-classification method was implemented to compare the LULC at these different times after two independent image classifications. Therefore, LULC change can be detected using two classified images by computing a matrix of change without the serious impact of atmospheric and environmental differences between the acquisition dates (Mas, 1999; Singh, 1989). The post-classification computation was performed on QGIS 3.4 and the Semi-Automatic Classification Plugin (SCP) in order to extract the LULC gains and losses.

One of the most important QGIS plugins is the SCP, which has been used by several scholars for their remote sensing applications (Marzouki & Dridri, 2022; Revuelta-Acosta et al., 2022; Simpson et al., 2021). The SCP allows the statistical evaluation of the maps produced. In the post-processing module of SCP, there is a land cover change function that enables the comparison of two classified images in order to assess LULC changes. The output classified images were downloaded from GEE and inserted into SCP to generate the file of LULC statistics (Congedo, 2021). The SCP is a Python-based plugin, and it extracts the LULC change by converting two classified LULC images into NumPy arrays and performing pixel-wise differentiation of these two arrays.

## Results

A total of 2000 pixels were captured across the 5 classes in both image composites, resulting in 1400 training data pixels and 600 validation data pixels. Table 3 shows the confusion matrices of observed versus predicted class values using the validation data for the images of 2017 and 2021. The classifier achieved an OA of 90% and Cohen's kappa of 0.88 for the 2017 composite, and an OA of 91% and Cohen's kappa of 0.89 for the 2021 composite. The UA for each class ranged from 83–100% in 2017

**Table 3** Confusion matrices for 2017 and 2021 composites based on classifier predictions (left) versus validation data (top)

		Artificial surfaces	Agricultural areas	Forests	Water bodies	Barren lands	Total	User's accuracy (%)
Composite of 2017	Artificial surfaces	104	16	0	0	0	120	87
	Agricultural areas	4	100	4	0	12	120	83
	Forests	0	0	112	0	8	120	93
	Water bodies	0	0	0	120	0	120	100
	Barren lands	0	12	4	0	104	120	87
	Total	108	128	120	120	124	600	
	Producer's accuracy (%)	96	78	93	100	84		
Composite of 2021	Artificial surfaces	116	4	0	0	0	120	97
	Agricultural areas	0	104	0	0	16	120	87
	Forests	0	0	116	0	4	120	97
	Water bodies	0	0	0	120	0	120	100
	Barren lands	0	8	20	0	92	120	77
	Total	116	116	136	120	112	600	
	Producer's accuracy (%)	100	90	85	100	82		

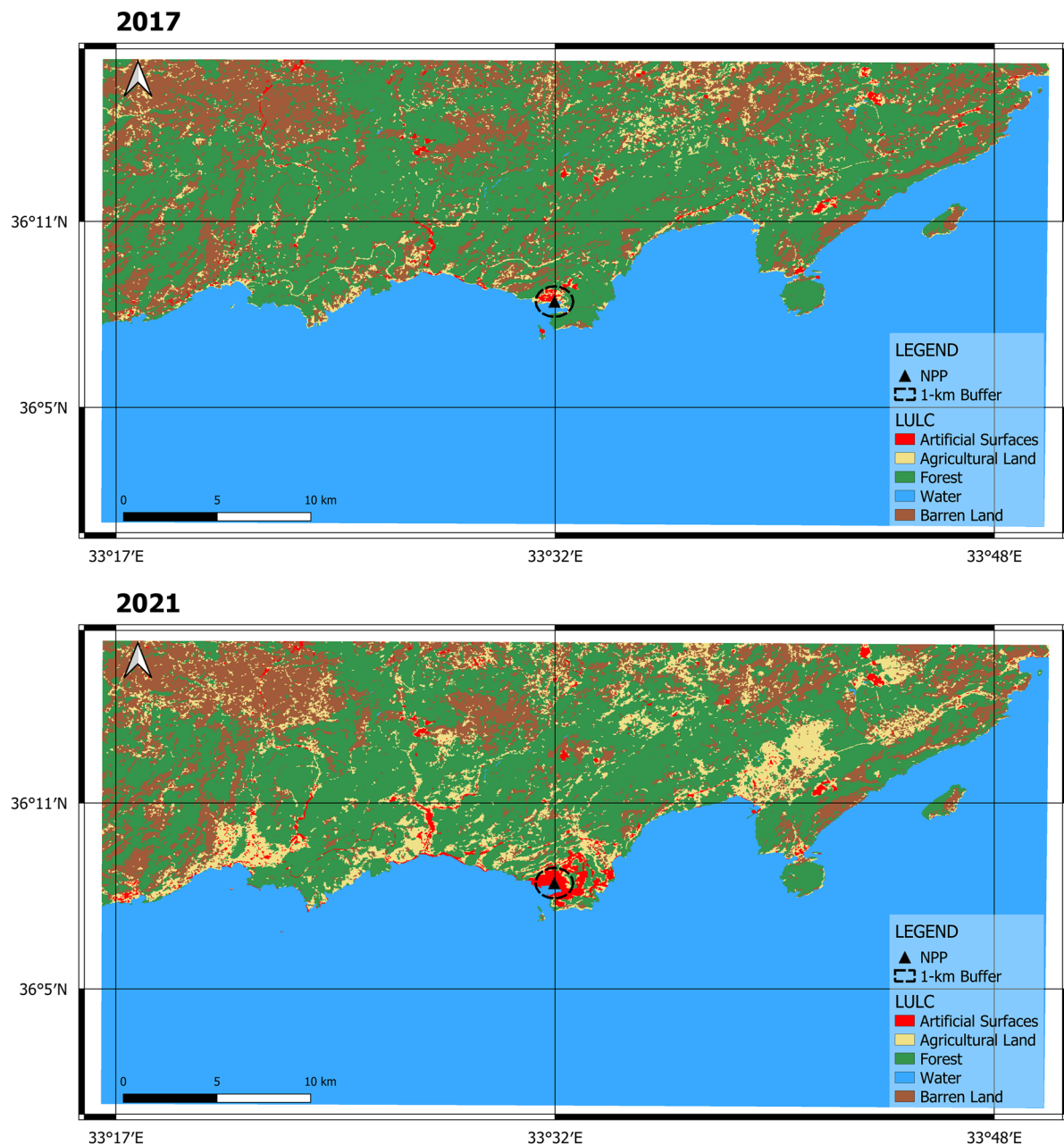
to 77–100% in 2021. Moreover, class-specific PA ranged from 78–100% for 2017 to 82–100% for 2021. Water bodies appeared to be the most accurately predicted, with UA and PA of 100% in both images. Agricultural areas were least accurately classified in the image of 2017 with UA and PA of 83% and 78%, respectively. Barren lands were the least accurate class in the image of 2021 with UA and PA of 77% and 82%, respectively.

Figure 3 demonstrates LULC predicted maps that consist of five classes (artificial surfaces, agricultural areas, forests, bare soil, water bodies, and barren lands) for 2017 and 2021 were generated based on the RF classification model. The LULC change analysis showed that (Table 4) the artificial surface class had the highest relative increase from 2017 to 2021 (78.46%), while there was a significant decrease in forests (−8.31%) and barren lands (−6.11%) in the whole study area. Looking at the 1 km buffer perimeter of the power plant, it was observed that the LULC change followed a different trend and the artificial surfaces had a much more serious increase (113.94%), while the areas covered by forests and barren lands decreased significantly (−69.13% and −74.28%, respectively). There is a loss of water bodies of up to 25.20% in the proximity of the Akkuyu NPP. In the whole study area and the proximity of the NPP, the surfaces covered by agricultural areas increased more than 45%.

Changes in each LULC class from 2017 to 2021 are shown in Fig. 4. In the whole study area (Fig. 4a), a large portion of agricultural areas was converted into other LULC classes: 9.1% to artificial surfaces, 27.6% to barren lands, and 21.7% to the forest. A small portion of forest lands was opened to agricultural lands (8.0%), and another portion was converted into barren lands (9.4%) and artificial surfaces (1.1%). Moreover, 0.5% of the bodies of water were turned into artificial surfaces. In the 1 km buffer perimeter of the Akkuyu NPP construction (Fig. 4b), the increase in the size of artificial surfaces was more striking. The construction activities around Akkuyu Bay converted 36.1% of agricultural lands, 54.1% of forests, and 23.2% of barren lands into artificial surfaces. Furthermore, the filling activities on the seashore resulted in a loss of water bodies of up to 26.5%.

## Discussions

LULC mapping and change detection analysis have generally been time-consuming and labor-intensive operations, and they are one of the primary research issues in RS applications. Recent developments in RS, along with the availability of open access data, have produced data that may be utilized for a variety of environmental monitoring applications. The GEE is becoming a more prominent tool for extracting



**Fig. 3** Model predicted LULC maps for 2017 and 2021 over the Akkuyu region

and classifying open-access satellite imagery. Here, we presented a case study to quantify regional LULC change using GEE and Landsat satellite observations. This study supports the use of GEE to collect the imagery data easily and implement classification procedures with GEE's built-in functions. We used the RF algorithm to classify LULC classes using 1400

training and 600 validation pixels for two composite images, and the performance of the classification was good enough to generate the LULC maps (with kappa scores of more than 0.88). In this respect, we created LULC maps for the Akkuyu region near an NPP construction site for the years 2017 and 2021, demonstrating that the LULC in the region has altered drastically

**Table 4** LULC change between 2017 and 2021

		2017 Area (km <sup>2</sup> )	2021 Area (km <sup>2</sup> )	Class change (km <sup>2</sup> )	Class change (%)
<b>Whole study area</b>	<b>Artificial surfaces</b>	2.16	3.85	+ 1.69	+ 78.46
	<b>Agricultural areas</b>	14.63	21.74	+ 7.11	+ 48.60
	<b>Forests</b>	76.63	70.26	- 6.37	- 8.31
	<b>Water bodies</b>	170.00	169.80	- 0.20	- 0.12
	<b>Barren lands</b>	36.58	34.35	- 2.23	- 6.11
	<b>Sum</b>	300	300	0	0
<b>1-km circle buffer around the NPP</b>	<b>Artificial surfaces</b>	0.90	1.93	+ 1.03	+ 113.94
	<b>Agricultural areas</b>	0.24	0.34	+ 0.11	+ 45.03
	<b>Forests</b>	0.81	0.25	- 0.56	- 69.13
	<b>Water bodies</b>	0.63	0.47	- 0.16	- 25.20
	<b>Barren lands</b>	0.56	0.14	- 0.42	- 74.28
	<b>Sum</b>	3.14	3.14	0	0

over the study period. The results indicated that the area covered by artificial surfaces showed an increasing trend during the study period.

According to the quantitative results of the LULC mapping with the RS approach, the natural land cover has been lost, while built-up areas (larger roads, new development areas) have significantly increased since the beginning of the construction of the Akkuyu NPP. The increase in roads might have direct effects on habitats and ecosystems and fragment natural land cover (Demirel et al., 2008). The villages around the construction site seem to have expanded in parallel with the roads. The construction itself has consumed hectares of barren lands, agricultural lands, and forests. The LULC change analysis clearly showed that the current land use preferences in the region contradict the issues and concerns mentioned in the existing body of literature (Janssen, 1984; Nero et al., 1977; Odum, 1976).

Even though NPPs may occupy a small amount of land, they can have far-reaching landscape effects (Wachs & Engel, 2021). According to the findings obtained from this study, it is seen that Akkuyu NPP caused landscape destruction in a wide area. The construction has expanded into the forests and barren lands. In Turkey, forests are protected by law. Forests in Turkey are generally used for timber production or maintained for the protection of catchment areas and wildlife habitats. However, if forests need to be used for settlements or other land uses, the government announces that these areas have “scientifically lost

their forest status” in order to use them for non-forest land use (Iban & Aksu, 2020). Conversely, construction has cleared the forest areas to a certain degree in the Akkuyu Bay without permission, and the degree of deforestation that may occur due to prospective development areas is not certain. In addition, deforestation can have adverse effects on local climate warming and decentralize nomads living in the forests. Furthermore, the ELUP and URAP documents do not indicate any land use policy for new transmission lines. If these lines pass through agricultural lands, these lands may be subject to expropriation or restrictive easements after the NPP becomes operative. As was determined from the LULC analysis, the Akkuyu NPP project has used sea surfaces. In addition, the ELUP legalizes new development areas on the seashores. The Akkuyu region is an important site for the preservation and reproduction of vulnerable and endangered species (i.e., monk seals and sea turtles), and such enlargement may have some negative effects on these species due to the construction, artificial lighting, higher marine traffic, and increases in water temperatures (Wang et al., 2008).

Expected policy outcomes should be to limit new development that may attract migration and keep the population density under a certain level around an NPP. However, the increase in artificial surfaces addresses new development areas and roads around rural villages. The authorities should preserve the rural characteristics of the region in order to enable rural communities to sustain their productivity. On the other hand, as Nero et al.

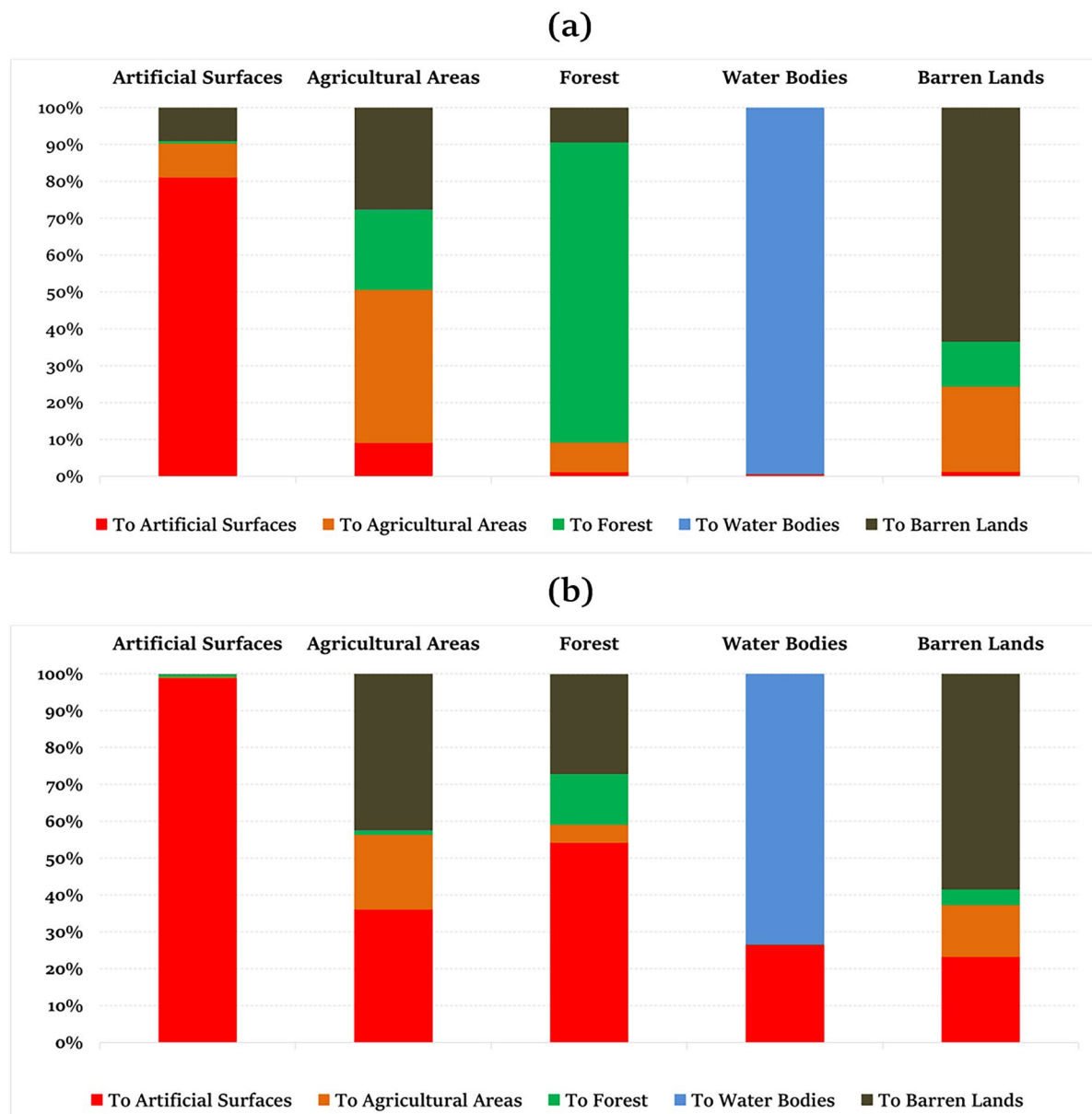


**Fig. 4** Change of each LULC class from 2017 to 2021: **a** the whole study area, **b** a 1-km circle buffer around the NPP

(1977) indicate, the authorities need to prepare action and emergency plans for exclusionary and low-populated zones around the NPPs. The concentration of the residential areas around the NPPs can bring chaos due to the lack of such a plan during a possible accident. For instance, Harrisburg City and Middletown were the closest urban areas to Three Mile Island NPP. During the meltdown in 1979, as summarized by Thornburgh (1987), the former governor of Pennsylvania, the company representatives,

and local administrators were unable to organize a massive evacuation in a short time. Such a massive evacuation can also be harmful to local residents. The Three Mile Island accident is one of the most striking examples of the negative consequences of the increase in urban living spaces in the vicinity of NPPs. The housing production around the NPPs should be reserved only for meeting the shelter and living needs of the plant workers. No new urban development should be allowed beyond this.

Nonetheless, according to our quantitative analysis, the new NPP construction seems to accelerate urbanization in the area. As Aydin (2020) states, since the need for the service sector has increased with the increase in the population, the number of people coming to this region to work has also increased. The increase in the population and number of residences around NPPs show us that the people in this region do not see NPPs as a risk and do not refrain from living around them. A similar finding was found by Clark et al. (1997) for residential areas around two NPPs in California. The study reported that the construction of NPPs did not create a negative image and did not cause a significant decrease in housing prices. However, once a nuclear disaster happens, the anthropomorphic activities stop around the NPPs, as reported by Ishihara and Tadono (2017) and Sekizawa et al. (2015). These studies reported that the people around Fukushima left the agricultural production, and there has not been any reconstruction in the region. In light of the literature summary, it is understood that people moved to the areas intensively during the construction of the NPPs, and the administrators did not seriously restrict these population movements. However, after the nuclear accidents, the evacuation plans of these settlements did not work sufficiently, and the regions were closed to settlement due to radioactive contamination. In this context, land use policies for NPPs are determined by the reality of the accident, not the probability of the accident.

The CEO of the APC states that the Akkuyu NPP is going to be the largest nuclear energy production site in the world and it will become fully operational by 2026 (World Nuclear News, 2021a). Even though the IAEA found that Turkish institutions and the APC implemented an adequate and satisfactory framework for nuclear security (World Nuclear News, 2021b), the Akkuyu Project will cause more people to accumulate in the study area and to live there permanently. However, there is no clear policy on how to protect the new settlements and how to evacuate the people living there in the event of a possible emergency. Thanks to this study, it is seen that the project site and the surrounding areas were opened to settlements in an uncontrolled manner and lost their natural characteristics. The ELUP supports this urban sprawl in the region. This plan does not contain any action, idea, or thought regarding the protection of natural habitats around the NPP. Turkey needs to review its land use and population density control policies and implement land use plans in line with the standards.

This revision should be made for both the first NPP in Akkuyu and the other two NPP projects Turkey plans to build in the future.

This study highlights the importance of monitoring LULC changes around NPPs and recommends the use of satellite images in this regard. The LULC monitoring using satellite images gave valuable information to manage the post-disaster LULC changes after the Fukushima Daiichi NPP disaster (Ishihara & Tadono, 2017; Sekizawa et al., 2015). The natural land cover changes and population dynamics created by the NPPs, which are under construction or have started their activities in different parts of the world, are still an issue that needs to be continuously examined by scholars. In order to achieve this, the data to be collected from the field and satellite images should be examined by considering social and environmental indicators. In this way, it will be easier for scientists to define the constraints of natural and human geography and to provide consultancy to decision-makers and companies that wish to use nuclear energy. As a result, it is critical to continuously monitor changes in LULC, which can be used in site selection research as well as in the preparation of action and emergency plans.

Certainly, this study has some limitations. Firstly, this study neither covers natural hazard scenarios nor physical or cyber security of the Akkuyu NPP. Some recent studies clarified these issues (Bıçakçı & Evren, 2022; Yavuz, 2022). Secondly, such a study may require higher spatial resolution in order to track the more detailed LULC classes. Thirdly, the census data was not used. Population growth and enlargement of residential areas are correlated with the LULC analysis obtained by the classification of satellite images only. Future studies will attempt to overcome these limitations.

## Conclusions

LULC change analysis of the construction site and its surroundings of the Akkuyu Nuclear Power Plant project in southern Turkey was undertaken in this case study, which was supported by remotely sensed Landsat 8 images. Five LULC classes (agricultural lands, artificial surfaces, barren lands, water bodies, and forests) were selected for the classification of satellite images on the study site. The composite images compiled in

2017 for the period before the construction of the project and the composite image compiled for 2021 reflecting the recent past were prepared on the Google Earth Engine platform, which enables easy management of open-access satellite images. For both images, 2000 sample pixels belonging to five LULC classes were created. Seventy percent of these sample pixels were used to train the classifier model, and the remaining 30% were used to assess the performance of the model. The Random Forest algorithm, which has given very successful results in the remote sensing literature, was used as the classifier model. As a result of training and validating the model, high classification performance was obtained for both images ( $\kappa > 0.88$ ). After the classification process, LULC maps for the years 2017 and 2021 were generated. In order to understand the LULC change between these two maps, statistical calculations for the LULC change were computed using the Semi-Automatic Classification Plugin on QGIS. While making these LULC change computations, both the entire study area ( $15 \times 25$  km) and a buffer zone with a radius of 1 km, which is the heart of the NPP construction, were taken into consideration. From 2017 to 2021 in the whole study area, the artificial surface class saw the greatest rise (78.46%), whereas forests ( $-8.31\%$ ) and barren lands experienced considerable decreases ( $-6.11\%$ ). When the 1 km buffer perimeter of the power plant was examined, it was determined that the LULC change followed a distinct trend, with artificial surfaces increasing greatly (113.94%), while the regions covered by forests and barren lands fell dramatically ( $-69.13\%$  and  $-74.28\%$ , respectively). A considerable proportion of agricultural areas in the study area were changed into other LULC classes: 9.1% to artificial surfaces, 27.6% to barren lands, and 21.7% to the forest. The rise in the area of artificial surfaces was especially noticeable within the 1 km buffer zone of the Akkuyu NPP installation. Around Akkuyu Bay, construction activities changed 36.1% of agricultural fields, 54.1% of forested lands, and 23.2% of barren lands into artificial surfaces. Furthermore, filling activities on the coastline resulted in a loss of up to 26.5% of water bodies.

As a result of this analysis, it was determined that in the last 4 years, built-up areas in the close vicinity of the Akkuyu NPP construction had increased, the forest areas had been severely damaged, the sea areas had been filled to a certain extent, and the agricultural lands had not been significantly affected. The figures and tables provided throughout the study show how

the LULC classes have evolved on the construction site and in the region. The construction of the Akkuyu NPP has caused a serious LULC conversion in its immediate vicinity. The main concern of this article is to examine the potential LULC change and population growth that this project will create in the region. Such analyses need to be sustained until the Akkuyu NPP is fully operational, with more ground-truthing and perhaps with different datasets with better spatial resolution. However, the construction site is restricted to the public and researchers, and the extent of the construction site is still unknown.

The number of studies conducted on the monitoring of population density and land use around NPPs is very limited. At the same time, few studies have been conducted on operating power plants. In countries that do not have experience in nuclear energy production, such as Turkey, it is important to research on this subject, to ensure that the country in question can monitor the environmental and social indicators around NPPs and determine how ready it is for possible emergency scenarios in accordance with the literature and international documents.

**Acknowledgements** We thank the handling editor and two anonymous reviewers for their constructive contributions and the time they have spent on this article. We are thankful to the Landsat Data Continuity Mission (LDCM) and Google Earth Engine development teams for providing valuable millions of open-access datasets for research. We would like to thank Dr. Luca Congedo for developing the Semi-Automatic Classification Plugin. We would like to thank Prof. Dr. Murat Yakar for setting up the Department of Remote Sensing and GIS at Mersin University from ground zero, and give the authors the opportunity of co-operating.

**Data availability** The datasets generated during and/or analyzed during the current study are available from the corresponding author on reasonable request.

## Declarations

**Conflict of interest** The authors declare no competing interests.

## References

- Abudeif, A. M., Abdel Moneim, A. A., & Farrag, A. F. (2015). Multicriteria decision analysis based on analytic hierarchy process in GIS environment for siting nuclear power plant in Egypt. *Annals of Nuclear Energy*, 75, 682–692. <https://doi.org/10.1016/j.anucene.2014.09.024>

- Adhikary, P. P., Barman, D., Madhu, M., Dash, Ch. J., Jakhar, P., Hombegowda, H. C., Naik, B. S., Sahoo, D. C., & Beer, K. (2019). Land use and land cover dynamics with special emphasis on shifting cultivation in Eastern Ghats Highlands of India using remote sensing data and GIS. *Environmental Monitoring and Assessment*, 191(5), 315. <https://doi.org/10.1007/s10661-019-7447-7>
- Ağbulut, Ü., Ceylan, İ., Gürel, A. E., & Ergün, A. (2019). The history of greenhouse gas emissions and relation with the nuclear energy policy for Turkey. *International Journal of Ambient Energy*. <https://doi.org/10.1080/01430750.2018.1563818>
- Akin, A., Sunar, F., & Berberoğlu, S. (2015). Urban change analysis and future growth of Istanbul. *Environmental Monitoring and Assessment*, 187(8), 506. <https://doi.org/10.1007/s10661-015-4721-1>
- Aksu, O., & Iban, M. C. (2019). Considerations on the land management system approach in Turkey by the experiences of a case study. *Survey Review*, 51(364), 87–96. <https://doi.org/10.1080/00396265.2017.1383711>
- Aydin, C. İ. (2020). Nuclear energy debate in Turkey: Stakeholders, policy alternatives, and governance issues. *Energy Policy*, 136(January 2019), 111041. <https://doi.org/10.1016/j.enpol.2019.111041>
- Barnthouse, L. W. (2013). Impacts of entrainment and impingement on fish populations: A review of the scientific evidence. *Environmental Science & Policy*, 31, 149–156. <https://doi.org/10.1016/j.envsci.2013.03.001>
- Biçakçı, A. S., & Evren, A. G. (2022). Thinking multiculturality in the age of hybrid threats: Converging cyber and physical security in Akkuyu nuclear power plant. *Nuclear Engineering and Technology*. <https://doi.org/10.1016/j.net.2022.01.033>
- Bilgilioğlu, S. S. (2022). Site selection for radioactive waste disposal facility by GIS based multi criteria decision making. *Annals of Nuclear Energy*, 165, 108795. <https://doi.org/10.1016/j.anucene.2021.108795>
- Bond, A., Palerm, J., & Haigh, P. (2004). Public participation in EIA of nuclear power plant decommissioning projects: A case study analysis. *Environmental Impact Assessment Review*, 24(6), 617–641. <https://doi.org/10.1016/j.eiar.2004.02.002>
- Çakır, G., Sivrikaya, F., & Keleş, S. (2008). Forest cover change and fragmentation using Landsat data in Maçka State Forest Enterprise in Turkey. *Environmental Monitoring and Assessment*, 137(1–3), 51–66. <https://doi.org/10.1007/s10661-007-9728-9>
- Celik, T. (2009). Unsupervised change detection in satellite images using principal component analysis and k-means clustering. *IEEE Geoscience and Remote Sensing Letters*, 6(4), 772–776. <https://doi.org/10.1109/LGRS.2009.2025059>
- Chirici, G., Mura, M., McInerney, D., Py, N., Tomppo, E. O., Waser, L. T., Travaglini, D., & McRoberts, R. E. (2016). A meta-analysis and review of the literature on the k-nearest neighbors technique for forestry applications that use remotely sensed data. *Remote Sensing of Environment*, 176, 282–294. <https://doi.org/10.1016/j.rse.2016.02.001>
- Clark, D. E., Michelbrink, L., Allison, T., & Metz, W. C. (1997). Nuclear power plants and residential housing prices. *Growth and Change*, 28(4), 496–519. <https://doi.org/10.1111/1468-2257.00069>
- Çolak, E., Chandra, M., & Sunar, F. (2021). The use of Sentinel 1/2 vegetation indexes with GEE time series data in detecting land cover changes in the Sinop nuclear power plant construction site. *The International Archives of the Photogrammetry, Remote Sensing and Spatial Information Sciences*, XLIII-B3-2021, 701–706. <https://doi.org/10.5194/isprs-archives-XLIII-B3-2021-701-2021>
- Congedo, L. (2021). Semi-Automatic Classification Plugin: A Python tool for the download and processing of remote sensing images in QGIS. *Journal of Open Source Software*, 6(64), 3172. <https://doi.org/10.21105/joss.03172>
- Demirel, H., Sertel, E., Kaya, S., & Zafer Seker, D. (2008). Exploring impacts of road transportation on environment: A spatial approach. *Desalination*, 226(1–3), 279–288. <https://doi.org/10.1016/j.desal.2007.02.111>
- Dewan, A. M., & Yamaguchi, Y. (2009). Using remote sensing and GIS to detect and monitor land use and land cover change in Dhaka Metropolitan of Bangladesh during 1960–2005. *Environmental Monitoring and Assessment*, 150(1–4), 237–249. <https://doi.org/10.1007/s10661-008-0226-5>
- Doygun, H., & Alphan, H. (2006). Monitoring urbanization of İskenderun, Turkey, and its negative implications. *Environmental Monitoring and Assessment*, 114(1–3), 145–155. <https://doi.org/10.1007/s10661-006-2524-0>
- Dubovyk, O., Menz, G., Conrad, C., Kan, E., Machwitz, M., & Khamzina, A. (2013). Spatio-temporal analyses of crop-land degradation in the irrigated lowlands of Uzbekistan using remote-sensing and logistic regression modeling. *Environmental Monitoring and Assessment*, 185(6), 4775–4790. <https://doi.org/10.1007/s10661-012-2904-6>
- Eisavi, V., Homayouni, S., Yazdi, A. M., & Alimohammadi, A. (2015). Land cover mapping based on random forest classification of multitemporal spectral and thermal images. *Environmental Monitoring and Assessment*, 187(5), 291. <https://doi.org/10.1007/s10661-015-4489-3>
- Ekmekçioğlu, M., Can Kutlu, A., & Kahraman, C. (2011). A fuzzy multi-criteria SWOT analysis: An application to nuclear power plant site selection. *International Journal of Computational Intelligence Systems*, 4(4), 583–595. <https://doi.org/10.1080/18756891.2011.9727814>
- Erdogán, M., & Kaya, İ. (2016). A combined fuzzy approach to determine the best region for a nuclear power plant in Turkey. *Applied Soft Computing*, 39, 84–93. <https://doi.org/10.1016/j.asoc.2015.11.013>
- Fallati, L., Savini, A., Sterlacchini, S., & Galli, P. (2017). Land use and land cover (LULC) of the Republic of the Maldives: First national map and LULC change analysis using remote-sensing data. *Environmental Monitoring and Assessment*, 189(8), 417. <https://doi.org/10.1007/s10661-017-6120-2>
- Foley, J. A. (2005). Global consequences of land use. *Science*, 309(5734), 570–574. <https://doi.org/10.1126/science.1111772>
- Gemitz, A. (2020). Are vegetation dynamics impacted from a nuclear disaster? The case of Chernobyl using remotely sensed NDVI and land cover data. *Land*, 9(11), 433. <https://doi.org/10.3390/land9110433>
- Ghosh, A., Sharma, R., & Joshi, P. K. (2014). Random forest classification of urban landscape using Landsat archive and ancillary data: Combining seasonal maps with decision level fusion. *Applied Geography*, 48, 31–41. <https://doi.org/10.1016/j.apgeog.2014.01.003>

- Gorelick, N., Hancher, M., Dixon, M., Ilyushchenko, S., Thau, D., & Moore, R. (2017). Google Earth Engine: Planetary-scale geospatial analysis for everyone. *Remote Sensing of Environment*, 202(2016), 18–27. <https://doi.org/10.1016/j.rse.2017.06.031>
- Guerrero, J. V. R., Escobar-Silva, E. V., Chaves, M. E. D., Mataveli, G. A. V., Bourscheidt, V., de Oliveira, G., Picoli, M. C. A., Shimabukuro, Y. E., & Moschini, L. E. (2020). Assessing land use and land cover changes in the direct influence zone of the Braço Norte Hydropower Complex. *Brazilian Amazonia. Forests*, 11(9), 1–13. <https://doi.org/10.3390/f11090988>
- Güler, M., Yomralioğlu, T., & Reis, S. (2007). Using Landsat data to determine land use/land cover changes in Sam-sun, Turkey. *Environmental Monitoring and Assessment*, 127(1–3), 155–167. <https://doi.org/10.1007/s10661-006-9270-1>
- Hawash, E., El-Hassanin, A., Amer, W., El-Nahry, A., & Effat, H. (2021). Change detection and urban expansion of Port Sudan, Red Sea, using remote sensing and GIS. *Environmental Monitoring and Assessment*, 193(11), 723. <https://doi.org/10.1007/s10661-021-09486-0>
- Hernandez, R. R., Hoffacker, M. K., Murphy-Mariscal, M. L., Wu, G. C., & Allen, M. F. (2015). Solar energy development impacts on land cover change and protected areas. *Proceedings of the National Academy of Sciences*, 112(44), 13579–13584. <https://doi.org/10.1073/pnas.1517656112>
- Hickey, S. M., Malkawi, S., & Khalil, A. (2021). Nuclear power in the Middle East: Financing and geopolitics in the state nuclear power programs of Turkey, Egypt, Jordan and the United Arab Emirates. *Energy Research & Social Science*, 74, 101961. <https://doi.org/10.1016/j.erss.2021.101961>
- Hu, H., Liu, W., & Cao, M. (2008). Impact of land use and land cover changes on ecosystem services in Menglun, Xishuangbanna. *Southwest China. Environmental Monitoring and Assessment*, 146(1–3), 147–156. <https://doi.org/10.1007/s10661-007-0067-7>
- Huang, C., Davis, L. S., & Townshend, J. R. G. (2002). An assessment of support vector machines for land cover classification. *International Journal of Remote Sensing*, 23(4), 725–749. <https://doi.org/10.1080/01431160110040323>
- IAEA. (2015). General safety requirements no.7—Preparedness and response for a nuclear or radiological emergency.
- IAEA. (2020). Country nuclear power profiles: Turkey. Retrieved September 3, 2022, from <https://cnpp.iaea.org/countryprofiles/Turkey/Turkey.htm>
- Iban, M. C., & Aksu, O. (2020). A model for big spatial rural data infrastructure in Turkey: Sensor-driven and integrative approach. *Land Use Policy*, 91, 104376. <https://doi.org/10.1016/j.landusepol.2019.104376>
- Ishihara, M., & Tadono, T. (2017). Land cover changes induced by the great east Japan earthquake in 2011. *Scientific Reports*, 7(1), 45769. <https://doi.org/10.1038/srep45769>
- Janssen, A. H. M. (1984). Nuclear power and land-use planning in the Netherlands. In *Energy Policy and Land-Use Planning* (pp 167–191). Elsevier. <https://doi.org/10.1016/B978-0-08-026757-9.50016-7>
- Karan, S. K., & Samadder, S. R. (2016). Accuracy of land use change detection using support vector machine and maximum likelihood techniques for open-cast coal mining areas. *Environmental Monitoring and Assessment*, 188(8), 486. <https://doi.org/10.1007/s10661-016-5494-x>
- Kavzoglu, T., & Colkesen, I. (2009). A kernel functions analysis for support vector machines for land cover classification. *International Journal of Applied Earth Observation and Geoinformation*, 11(5), 352–359. <https://doi.org/10.1016/j.jag.2009.06.002>
- Kharazmi, R., Tavili, A., Rahdari, M. R., Chaban, L., Panidi, E., & Rodrigo-Comino, J. (2018). Monitoring and assessment of seasonal land cover changes using remote sensing: A 30-year (1987–2016) case study of Hamoun Wetland. *Iran. Environmental Monitoring and Assessment*, 190(6), 356. <https://doi.org/10.1007/s10661-018-6726-z>
- Kidane, Y., Stahlmann, R., & Beierkuhnlein, C. (2012). Vegetation dynamics, land use and land cover change in the Bale Mountains. *Ethiopia. Environmental Monitoring and Assessment*, 184(12), 7473–7489. <https://doi.org/10.1007/s10661-011-2514-8>
- Kindu, M., Schneider, T., Teketay, D., & Knoke, T. (2015). Drivers of land use/land cover changes in Munessa-Shashemene landscape of the south-central highlands of Ethiopia. *Environmental Monitoring and Assessment*, 187(7), 452. <https://doi.org/10.1007/s10661-015-4671-7>
- Kirkwood, C. W. (1982). A case history of nuclear power plant site selection. *Journal of the Operational Research Society*, 33(4), 353–363. <https://doi.org/10.1057/jors.1982.77>
- Kusak, L., Unel, F. B., Alptekin, A., Celik, M. O., & Yakar, M. (2021). A priori association rule and K-means clustering algorithms for interpretation of pre-event landslide areas and landslide inventory mapping. *Open Geosciences*, 13(1), 1226–1244. <https://doi.org/10.1515/geo-2020-0299>
- Küçüköglu, S. (2020). *Multiple criteria decision making methods nuclear power plant site selection in Turkey*. Istanbul Commerce University M.Sc.
- Lee, J., Lee, J., Kim, K., & Lee, K. (2021). Change of NDVI by surface reflectance based on KOMPSAT-3/3A images at a zone around the Fukushima Daiichi Nuclear Power Plant. *Korean Journal of Remote Sensing*, 37(6\_3), 2027–2034.
- Lee, S.-H., Seo, H.-W., & Kim, C.-L. (2018). Preparation of radiological environmental impact assessment for the decommissioning of nuclear power plant in Korea. *Journal of the Nuclear Fuel Cycle and Waste Technology(JNFCWT)*, 16(1), 107–122. <https://doi.org/10.7733/jnfcwt.2018.16.1.107>
- Lele, N., & Joshi, P. K. (2009). Analyzing deforestation rates, spatial forest cover changes and identifying critical areas of forest cover changes in North-East India during 1972–1999. *Environmental Monitoring and Assessment*, 156(1–4), 159–170. <https://doi.org/10.1007/s10661-008-0472-6>
- Li, P., Jiang, L., & Feng, Z. (2013). Cross-comparison of vegetation indices derived from Landsat-7 enhanced thematic mapper plus (ETM+) and Landsat-8 operational land imager (OLI) sensors. *Remote Sensing*, 6(1), 310–329. <https://doi.org/10.3390/rs6010310>
- Lu, D., Mausel, P., Brondízio, E., & Moran, E. (2004). Change detection techniques. *International Journal of Remote Sensing*, 25(12), 2365–2401. <https://doi.org/10.1080/0143116031000139863>
- Lv, Z., Liu, T., Shi, C., Benediktsson, J. A., & Du, H. (2019). Novel land cover change detection method based on k-means

- clustering and adaptive majority voting using bitemporal remote sensing images. *IEEE Access*, 7, 34425–34437. <https://doi.org/10.1109/ACCESS.2019.2892648>
- Mahdavi Saeidi, A., Babaie Kafaky, S., & Mataji, A. (2020). Detecting the development stages of natural forests in northern Iran with different algorithms and high-resolution data from GeoEye-1. *Environmental Monitoring and Assessment*, 192(10), 653. <https://doi.org/10.1007/s10661-020-08612-8>
- Manfré, L. A., Cruz, B. B., & Quintanilha, J. A. (2020). Urban settlements and road network analysis on the surrounding area of the Almirante Alvaro Alberto Nuclear Complex, Angra dos Reis. *Brazil. Applied Spatial Analysis and Policy*, 13(1), 209–221. <https://doi.org/10.1007/s12061-019-09299-2>
- Marzouki, A., & Dridri, A. (2022). Normalized difference enhanced sand index for desert sand dunes detection using Sentinel-2 and Landsat 8 OLI data, application to the north of Figuig. *Morocco. Journal of Arid Environments*, 198, 104693. <https://doi.org/10.1016/j.jaridenv.2021.104693>
- Mas, J.-F. (1999). Monitoring land-cover changes: A comparison of change detection techniques. *International Journal of Remote Sensing*, 20(1), 139–152. <https://doi.org/10.1080/014311699213659>
- Melikoglu, M. (2016). The role of renewables and nuclear energy in Turkey's Vision 2023 energy targets: Economic and technical scrutiny. *Renewable and Sustainable Energy Reviews*, 62, 1–12. <https://doi.org/10.1016/j.rser.2016.04.029>
- NEI. (2015). Land needs for wind, solar dwarf nuclear plant's footprint. Retrieved September 3, 2022, from <https://www.nei.org/news/2015/land-needs-for-wind-solar-dwarf-nuclear-plants>
- Nero, A. V., Schroeder, C. H., & Yen, W. W. S. (1977). Control of population densities surrounding nuclear power plants. Retrieved September 3, 2022, from <https://escholarship.org/content/qt6nm4f8f8/qt6nm4f8f8.pdf>
- Odum, E. P. (1976). The ecosystem approach. In *Environmental Impact of Nuclear Power Plants* (pp 29–40). Elsevier. <https://doi.org/10.1016/B978-0-08-019956-6.50007-6>
- Pal, M. (2005). Random forest classifier for remote sensing classification. *International Journal of Remote Sensing*, 26(1), 217–222. <https://doi.org/10.1080/01431160412331269698>
- Pasqualetti, M. J., & Pijawka, K. D. (1996). Unsiting nuclear power plants: Decommissioning risks and their land use context. *Professional Geographer*, 48(1), 57–69. <https://doi.org/10.1111/j.0033-0124.1996.00057.x>
- Phan, T. N., Kuch, V., & Lehnert, L. W. (2020). Land cover classification using Google Earth Engine and random forest classifier—The role of image composition. *Remote Sensing*, 12(15), 2411. <https://doi.org/10.3390/rs12152411>
- Prabu, P., & Dar, M. A. (2018). Land-use/cover change in Coimbatore urban area (Tamil Nadu, India)—A remote sensing and GIS-based study. *Environmental Monitoring and Assessment*, 190(8), 445. <https://doi.org/10.1007/s10661-018-6807-z>
- Qiang, Y., & Lam, N. S. N. (2015). Modeling land use and land cover changes in a vulnerable coastal region using artificial neural networks and cellular automata. *Environmental Monitoring and Assessment*, 187(3), 57. <https://doi.org/10.1007/s10661-015-4298-8>
- Revuelta-Acosta, J. D., Guerrero-Luis, E. S., Terrazas-Rodriguez, J. E., Gomez-Rodriguez, C., & Alcalá Perea, G. (2022). Application of remote sensing tools to assess the land use and land cover change in Coatzacoalcos, Veracruz, Mexico. *Applied Sciences*, 12(4), 1882. <https://doi.org/10.3390/app12041882>
- Rezaeimahmoudi, M., Esmaeli, A., Gharegozlu, A., Shabanian, H., & Rokni, L. (2014). Application of geographical information system in disposal site selection for hazardous wastes. *Journal of Environmental Health Science and Engineering*, 12(1), 141. <https://doi.org/10.1186/s40201-014-0141-3>
- Sabuncu, A. (2020). Monitoring deforestation by multitemporal data using remote sensing technologies: A case study of Sinop-Turkey. *Fresenius Environmental Bulletin*, 29, 3827–3832.
- Sah, S., van Aardt, J. A. N., McKeown, D. M., & Messinger, D. W. (2012). A multi-temporal analysis approach for land cover mapping in support of nuclear incident response (S. S. Shen & P. E. Lewis, Eds.; pp 83900C-83900C – 7). <https://doi.org/10.1117/12.919276>
- Salter, I., Robinson, P., Freeman, M., & Jagasia, J. (2012). Environmental impacts and assessment in nuclear power programmes. Woodhead Publishing Limited. <https://doi.org/10.1533/9780857093776.2.567>
- Sano, E. E., Rosa, R., Brito, J. L. S., & Ferreira, L. G. (2010). Land cover mapping of the tropical savanna region in Brazil. *Environmental Monitoring and Assessment*, 166(1–4), 113–124. <https://doi.org/10.1007/s10661-009-0988-4>
- Sazib, N., Mladenova, I., & Bolten, J. (2018). Leveraging the Google Earth Engine for drought assessment using global soil moisture data. *Remote Sensing*, 10(8), 1265. <https://doi.org/10.3390/rs10081265>
- Sekertekin, A., Abdikan, S., & Marangoz, A. M. (2018). The acquisition of impervious surface area from LANDSAT 8 satellite sensor data using urban indices: A comparative analysis. *Environmental Monitoring and Assessment*, 190(7), 381. <https://doi.org/10.1007/s10661-018-6767-3>
- Sekizawa, R., Ichii, K., & Kondo, M. (2015). Satellite-based detection of evacuation-induced land cover changes following the Fukushima Daiichi nuclear disaster. *Remote Sensing Letters*, 6(11), 824–833. <https://doi.org/10.1080/2150704X.2015.1076207>
- Sesli, F. A., Karsli, F., Colkesen, I., & Akyol, N. (2009). Monitoring the changing position of coastlines using aerial and satellite image data: An example from the eastern coast of Trabzon, Turkey. *Environmental Monitoring and Assessment*, 153(1–4), 391–403. <https://doi.org/10.1007/s10661-008-0366-7>
- Shao, Y., & Lunetta, R. S. (2012). Comparison of support vector machine, neural network, and CART algorithms for the land-cover classification using limited training data points. *ISPRS Journal of Photogrammetry and Remote Sensing*, 70, 78–87. <https://doi.org/10.1016/j.isprsjprs.2012.04.001>
- Shelestov, A., Lavreniuk, M., Kussul, N., Novikov, A., & Skakun, S. (2017). Exploring Google Earth Engine platform for big data processing: Classification of multitemporal satellite imagery for crop mapping. *Frontiers in Environmental Science*, 5, 101. <https://doi.org/10.3389/fenvs.2017.00101>

- in *Earth Science*, 5(February), 1–10. <https://doi.org/10.3389/feart.2017.00017>
- Shetty, S. (2019). Analysis of machine learning classifiers for LULC classification on Google Earth Engine analysis of machine learning classifiers for LULC classification on Google Earth Engine. 1–65.
- Simpson, L. T., Cantz, S. W. J., Cissell, J. R., Steinberg, M. K., Cherry, J. A., & Feller, I. C. (2021). Bird rookery nutrient over-enrichment as a potential accelerator of mangrove cay decline in Belize. *Oecologia*, 197(3), 771–784. <https://doi.org/10.1007/s00442-021-05056-w>
- Sims, D. A., & Gamon, J. A. (2002). Relationships between leaf pigment content and spectral reflectance across a wide range of species, leaf structures and developmental stages. *Remote Sensing of Environment*, 81(2–3), 337–354. [https://doi.org/10.1016/S0034-4257\(02\)00010-X](https://doi.org/10.1016/S0034-4257(02)00010-X)
- Singh, A. (1989). Digital change detection techniques using remotely-sensed data. *International Journal of Remote Sensing*, 10(6), 989–1003. <https://doi.org/10.1080/01431168908903939>
- Singh, N. P., Mukherjee, T. K., & Shrivastava, B. B. P. (1997). Monitoring the impact of coal mining and thermal power industry on land use pattern in and around Singrauli Coal-field using remote sensing data and GIS. *Journal of the Indian Society of Remote Sensing*, 25(1), 61–72. <https://doi.org/10.1007/BF02995419>
- Song, X.-P., Hansen, M. C., Stehman, S. V., Potapov, P. V., Tyukavina, A., Vermote, E. F., & Townshend, J. R. (2018). Global land change from 1982 to 2016. *Nature*, 560(7720), 639–643. <https://doi.org/10.1038/s41586-018-0411-9>
- Tamiminia, H., Salehi, B., Mahdianpari, M., Quackenbush, L., Adeli, S., & Brisco, B. (2020). Google Earth Engine for geo-big data applications: A meta-analysis and systematic review. *ISPRS Journal of Photogrammetry and Remote Sensing*, 164, 152–170. <https://doi.org/10.1016/j.isprsjprs.2020.04.001>
- Tassi, A., & Vizzari, M. (2020). Object-oriented LULC classification in Google Earth Engine combining SNIC, GLCM, and machine learning algorithms. *Remote Sensing*, 12(22), 3776. <https://doi.org/10.3390/rs12223776>
- Thomas, S. (2018). Russia's nuclear export programme. *Energy Policy*, 121, 236–247. <https://doi.org/10.1016/j.enpol.2018.06.036>
- Thornburgh, R. (1987). The Three Mile Island experience: Ten lessons in emergency management. *Industrial Crisis Quarterly*, 1(1), 5–13. <https://doi.org/10.1177/108602668700100102>
- Turkish Ministry of Interior-Disaster and Emergency Management Presidency. (2019). *Ulusal Radyasyon Acil Durum Planı (URAP)*.
- Turner, B. L., Lambin, E. F., & Reenberg, A. (2007). The emergence of land change science for global environmental change and sustainability. *Proceedings of the National Academy of Sciences*, 104(52), 20666–20671. <https://doi.org/10.1073/pnas.0704119104>
- Wachs, E., & Engel, B. (2021). Land use for United States power generation: A critical review of existing metrics with suggestions for going forward. *Renewable and Sustainable Energy Reviews*, 143, 110911. <https://doi.org/10.1016/j.rser.2021.110911>
- Wang, Y.-S., Lou, Z.-P., Sun, C.-C., & Sun, S. (2008). Ecological environment changes in Daya Bay, China, from 1982 to 2004. *Marine Pollution Bulletin*, 56(11), 1871–1879. <https://doi.org/10.1016/j.marpolbul.2008.07.017>
- World Nuclear News. (2021a). Akkuyu construction to be completed by 2026, says project CEO. Retrieved September 3, 2022, from <https://www.world-nuclear-news.org/Articles/Akkuyu-fully-operational-by-2026--says-project>
- World Nuclear News. (2021b). IAEA completes security advisory mission in Turkey. Retrieved September 3, 2022, from <https://www.world-nuclear-news.org/Articles/IAEA-completes-security-advisory-mission-in-Turkey>
- Wu, Y., Li, S., & Yu, S. (2016). Monitoring urban expansion and its effects on land use and land cover changes in Guangzhou City. *China Environmental Monitoring and Assessment*, 188(1), 54. <https://doi.org/10.1007/s10661-015-5069-2>
- Xu, H., Zhang, B., & Liu, Y. (2021). New safety strategies for nuclear power plants: A review. *International Journal of Energy Research*, 45(8), 11564–11588. <https://doi.org/10.1002/er.6657>
- Yadav, B. K. V., & Nandy, S. (2015). Mapping aboveground woody biomass using forest inventory, remote sensing and geostatistical techniques. *Environmental Monitoring and Assessment*, 187(5), 308. <https://doi.org/10.1007/s10661-015-4551-1>
- Yamamoto, D., Feikens, J., & Haller, M. (2020). Nuclear-to-nature land conversion. *Geographical Review*, 00(00), 1–22. <https://doi.org/10.1080/00167428.2020.1799212>
- Yavuz, C. (2022). Distinctive stochastic tsunami hazard and environmental risk assessment of Akkuyu nuclear power plant by Monte Carlo simulations. *Arabian Journal for Science and Engineering*. <https://doi.org/10.1007/s13369-022-06938-8>
- Yin, J., Yin, Z., Zhong, H., Xu, S., Hu, X., Wang, J., & Wu, J. (2011). Monitoring urban expansion and land use/land cover changes of Shanghai metropolitan area during the transitional economy (1979–2009) in China. *Environmental Monitoring and Assessment*, 177(1–4), 609–621. <https://doi.org/10.1007/s10661-010-1660-8>
- Yousefi, S., Khatami, R., Mountrakis, G., Mirzaee, S., Pourghasemi, H. R., & Tazeh, M. (2015). Accuracy assessment of land cover/land use classifiers in dry and humid areas of Iran. *Environmental Monitoring and Assessment*, 187(10), 641. <https://doi.org/10.1007/s10661-015-4847-1>
- Zadbagher, E., Becek, K., & Berberoglu, S. (2018). Modeling land use/land cover change using remote sensing and geographic information systems: Case study of the Seyhan Basin, Turkey. *Environmental Monitoring and Assessment*, 190(8), 494. <https://doi.org/10.1007/s10661-018-6877-y>

**Publisher's Note** Springer Nature remains neutral with regard to jurisdictional claims in published maps and institutional affiliations.

Springer Nature or its licensor holds exclusive rights to this article under a publishing agreement with the author(s) or other rightsholder(s); author self-archiving of the accepted manuscript version of this article is solely governed by the terms of such publishing agreement and applicable law.